Atmospheric haze layers and brightness of the horizon

By FRIEDRICH E. VOLZ, *Astronomical Institute, Univerity of Tübingen, Germany*

(Publication No. 72)

(Manuscript received January 23, 1963; revised version February 22, 1964)

ABSTRACT

The optics of thin, extended haze layers in the atmosphere as viewed in a horizontal plane are investigated. First discussed are the geometry and brightness profile of an isolated layer, taking account of attenuation and different vertical distribution of the particles. The brightness of layers at altitudes of 22 and 3 km, embedded in a slightly turbid atmosphere, is calculated for solar elevation 20°, azimuths 0 and 180°, and wavelength 500 nm. An attempt is made to include multiple scattering. These results are compared with the effect on the brightness of the zenith and on a searchlight beam caused by a layer.

1. Introduction

From mountains, balloons and airplanes, haze tops and thin haze layers of large horizontal extention can often be observed in a horizontal direction. They are best seen if the observer is just at their top, or slightly higher. The layers are brightest, and sometimes slightly colored, near the sun's vertical, especially for low sun. At large azimuthal distance from the sun, they are brownish, grey, or whitish with little brightness contrast, mostly darker than the sky.

Visual observations of tropospheric haze layers, which usually occur just below a temperature inversion (including the tropopause) have been often described. According to LÖHLE (1940), sharp layers are characteristic of dry descending air masses of stable stratification, while dissolution and disappearance of layers is an indication of labilization and decay of high pressure cells.

Even in the stratosphere, thin dust layers have been relatively often observed. JACOBS (1954) reported a series of airplane observations of unusual strong layers at about 15 km altitude at the end of July 1953 over England. On high altitude balloon flights, SIMON (1958) and MOORE (personal communication, 1960) observed, particulary in the sun's azimuth, thin bands of haze or dust at 24 km. These observations were once surprising, but such stratospheric layers may be a common feature of the belt of submicroscopic particles extending from about 17 to 23 km, which has been measured recently by JUNGE, CHAGNON & MANSON (1961) and confirmed by sky brightness measurements (ROESSLER, 1961) and twilight observations (VOLZ & GOODY, 1962). Expecially interesting are the edge-on observation and identification of the night glow layer at about 100 km on manned orbital flights (CARPENTER, O'KEEFE & DUNKELMAN, 1962).

From the ground, high dust layers are recognized by visual, oblique observations only if their optical density varies, either by lateral inhomogeneity (isolated streakes and clouds of dust) or by undulatory height changes. As is well known from noctilucent clouds (LUDLAM, 1957), twilight conditions may promote the detectability of such layers. Accurate height determination requires photogrammetric methods. In a vertical searchlicht beam, only strong layers can show up because of the small backscatter by haze. Layers above the tropopause have been observed by this method by MOROZOV (1957) and DRIVING & SMIRNOVA (1958), and were discussed in relation to nacreous clouds.

Airborne measurements of volume scattering (WALDRAM, 1945) or of skylight brightness (e.g. TOUSEY & HULBERT, 1947; ROESSLER, 1961; MIKIROV, 1962) as function of height are also less sensitive to small, optically thin layers than observations of horizontal contrast (see sect. 4).

This short discussion of relevant observations shows that haze layers, especially thin and homogeneous ones, are best observed and investigated by their optical effects on the brightness of the horizon. Today's frequency and ceiling of airplanes permits regular study of such layers up the stratospheric heights. As will be shown, approximate data on thickness and optical density of the layers can be gathered by this method with little effort. Other aspects of the layers are relations to air masses and inversions, and the origin and nature of the particles causing them. Tropospheric haze layers may often be traced back to previous cloud layers with their complex influences on concentration and size distribution of nuclei (coagulation, and, probably most important, absorption of gas traces). But in haze layers of unknown relative humidity it will often be difficult to decide to what extent a layer is caused by a higher concentration (and different size distribution) of particles than in surrounding air, and to what extent by high humidity (precondensation). In the very dry upper atmosphere this problem may arise only with extremely low temperatures (nacreous and noctilucent clouds), so that the origin of layers observed under normal temperature conditions is very interesting. Volcanic eruptions—as in the case of the layers observed during the end of July 1953 (JACOBS, 1954)—und meteoric activity are hardly to be regular natural sources. More likely is a direct connection with Junge's stratospheric dust belt. Visual observations of such layers may be very important for studies of its temporal and spatial homogeneity.

A theoretical investigation related to our problem seems to have been made only by SIEDENTOPF (1948). He computed the brightness contrast between the clear sky and the top of a dense and deep haze layer along the horizon and finds a good agreement with visual observations.

2. Geometry and brightness of an isolated layer in the atmosphere

2.1. GEOMETRY AND PATH LENGTH

First we consider a layer in the atmosphere of infinite horizontal extention and thickness D, with the top at altitude H. Scattering and attenuation in the atmosphere are neglected, and even the layer is assumed to be optically thin. For lateral, airborne observations, the layer is mainly defined by the lines of sight tangent to the upper and lower boundaries of the layer (Fig. 1a). Neglecting refraction, their angular depressions with respect to the geometric horizon are

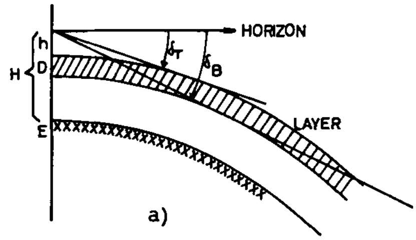

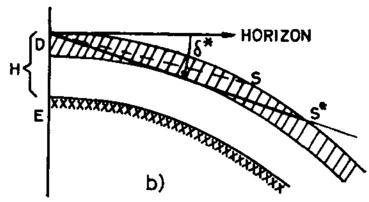

FIG. 1. Geometry of atmospheric layers. Observer above the layer (a) and at their top (b).

$$\delta_{\text{top}} = \sqrt{\frac{2h}{E+H}} \qquad h > 0 \tag{1 a}$$

and
$$\delta_{\text{bottom}} = \sqrt{\frac{2(h+D)}{E+H-D}} \qquad h \geqslant -D, \tag{1 b}$$

if the observer is at the altitude h above the top of the layer and E means the radius of the earth. In the most interesting case, with the observer at the top of the layer ($h=0$, Fig. 1b), we have

$$\delta_{\text{top}} = 0, \quad \delta_{\text{bottom}} - = \delta^* = \sqrt{\frac{2D}{E+H}}. \tag{2 a}$$

Then, the geometric path length S through the layer is a maximum in direction δ^* with the value

$$S^* = 2\sqrt{2D(E+H)} = 2\delta^*(E+H). \tag{2 b}$$

$S^*/2$ is the distance to the grazing point. Some values of δ^* and S^* are given in Table 1 as function of D.

Graphically obtained geometrical path lengths as function of depression are shown in Fig. 2

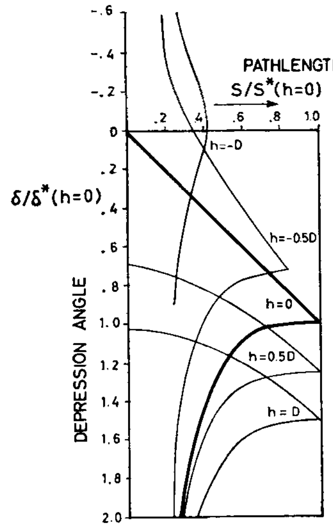

FIG. 2. Path length (S) or brightness of an isolated layer with rectangular particle distribution, as function of depression δ for different distance from top of layer (h) with respect to layer thickness (D).

for some altitudes h of the observer above the top of the layer with respect to the thickness of the layer. Path lengths as well as depressions are referred to S resp. to δ^* for $h = 0$. These path-length profiles are also brightness profiles, if the particle distribution in the layer is uniform between top and bottom, and if attenuation is neglected. If the observer is at the top of such

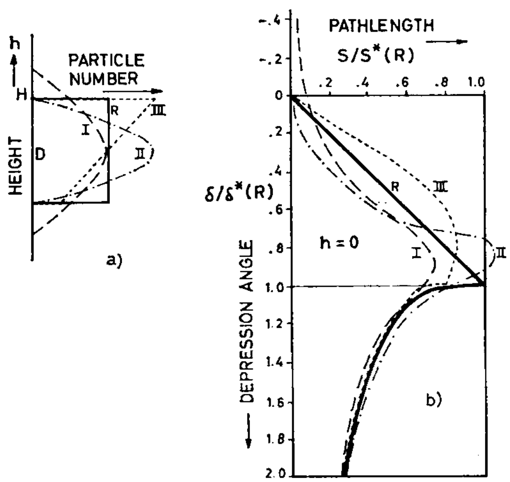

FIG. 3. Different assumptions on the vertical distribution of particle number (a), and resulting brightness profiles (b).

TABLE 1. *Maximum path length S^* and depression δ^* as function of layer thickness D.*

D(km)	δ^*(rad	δ^*(deg)	S^*(km)
0.01	0.0018	0.102°	22.4
0.1	0.0057	0.32°	70.8
1.0	0.018	1.02°	224
10.0	0.057	3.2°	708

a layer ($h = 0$), the path length or brightness increases linearly from horizontal direction to δ^*. Then follows a sharp decrease to a rather constant level. The top of the layer gives raise to a further discontinuity for an observer positioned above the layer (lower curves). But perceptability of a layer diminishes quickly if observations are made from within or below the layer because of the flattening brightness profile (top curves). This is well known by airborne observers, and also the difficulty to define the exact altitude of the top of the layer during ascend (i.e. the moment when $\delta = 0$; SIEDENTOPF, 1948).

It is noteworthy that the median altitude of a layer is of no importance to the direction of maximum path length. Also, the effective height of a layer obtained by vertical measurements, and the "altitude" of the layer derived from the depression angle of maximum brightness may differ by half the thickness of the layer (CARPENTER, O'KEEFE & DUNKELMAN, 1962).

2.2. INFLUENCE OF THE VERTICAL PARTICLE DISTRIBUTION

Atmospheric haze layers may seldom have a rectangular particle distribution as assumed in the model. The sharp discontinuity of the path-length profile is expected to disappear as the particle distribution smoothes. The same effect will occur if the thickness or height (by wavelike motions) of a layer of rectangular distribution varies in horizontal direction.

In Fig. 3 b, path-length profiles for two particle distributions (I and II in Fig. 3 a) similar to Gaussian distributions and for a trapezium distribution (III) are compared with the profile of the rectangular distribution (R). All distributions have the same total particle number. Path-length and depression angle of the profiles are referred to S^* and δ^* of profile

R. Profiles of Gauss-like distribution differ clearly from profile *R* and III for $\delta < \delta^*$, but differences are small for larger depressions. However, these models show that the results of the further investigations, which will be restricted to rectangular particle distributions, are characteristic for most possible distributions.

2.3. Brightness profile of an isolated sunlit haze layer, including attenuation

The brightness of an isolated, curved haze layer at depression δ is generally given by

$$\beta_L(\delta) = \int_0^{S(\delta)} F_{(s)}\sigma(\theta, s)e^{-\Sigma(s)S(d)}ds. \qquad (3)$$

This simplifies for a rectangular vertical particle distribution to

$$B_L(\delta) = F\sigma(\theta)S(\delta)\Sigma^{-1}(1 - e^{-\Sigma S(\delta)}), \qquad (3')$$

where F = illumination of the layer (e.g. by the sun) at distance s, $\sigma(\theta, s)$ = scattering coefficient for scattering angle θ per unit of path length ds and per radian (ω), $\Sigma(s) = \int_0^{s(\delta)} \sigma(\theta, s)d\omega$ (+ absorption coefficient) = total attenuation coefficient per ds.

Scattering phase function and attenuation coefficient are defined by concentration, size distribution, shape, and refractive index of the particles of the layer.

The brightness profiles given in Fig. 4 for layers with top at the altitude of the observer and with rectangular particle distribution are normalized to the brightness B^* in direction δ^* and for $\Sigma/S^* = 0$, i.e. for neglected attenuation. The table below Fig. 4 shows the values of Σ and of the visibility range $V = 3.92/\Sigma$ in terms of the maximum path length S^*, and the transmission T^* of the layer in direction δ^*. The characteristic shape of an optically thin layer is almost lost if V is larger than about 1.7 S^* because of the small contribution of distant parts of the layer. This shows that the layer could be largely distorted or even missing at $s \gtrsim 0.5\ S^*$ without much change of the brightness profile.

2.4. The relation of thickness and brightness of a layer

Now we are briefly considering the effects of change of the vertical thickness D of a layer

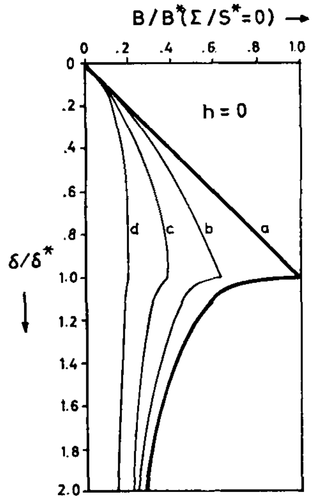

	a	b	c	d
Σ/S^*	0	1	2.3	5
V/S^*	∞	3.92	1.7	0.79
T^*	1,0	0.37	0.1	0.007

Fig. 4. Normalized brightness profiles for different attenuation.

on its brightness for two different conditions of particle density. In the first case, we assume the particle number in the vertical column of the layer to be independent of D, i.e. particle volume density or scattering coefficient $\sigma(D) \sim 1/D$. In the atmosphere, this may occur with up and down motions (compressions and dilutions) having no lateral component, or by an increase of D by turbulance. Neglecting attenuation and assuming conservation of the rectangular particle profile, the brightness in direction $\delta^*(\sim\sqrt{D})$ is, according to Eq. (3′), given by $B(\delta^*) \sim \sigma S^*$, so that with $\sigma(D) \sim 1/D$, and $S^* \sim \sqrt{D}$,

$$B(\delta^*, D) \sim 1/\sqrt{D}. \qquad (4)$$

As the thickness of the layer increases, its brightness decreases slowly in the corresponding direction δ^*.

Secondly, if the layer thickness is changing by corresponding change of particle number such that $\sigma(D)$ = const, we have

$$B(\delta^*, D) \sim \sqrt{D}. \qquad (4')$$

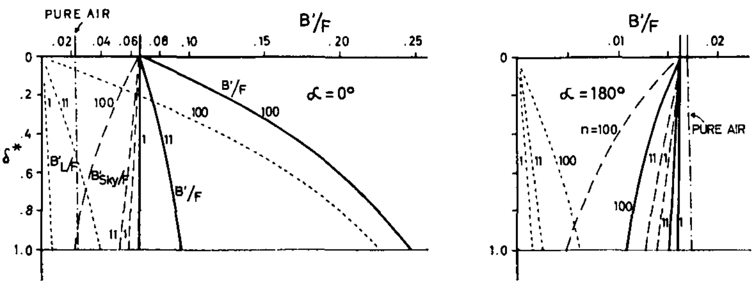

FIG. 5. Brightness profiles of a haze layer of 12.5 m thickness ($\delta^* = 0.11^\circ_2$) at 22 km altitude. Wavelength 500 nm, solar elevation 20°, azimuth 0 and 180°; primary scattering only. n is the ratio of aerosol density in the layer and in surrounding air. Dotted lines: brightness from region of layer (B'_L/F); broken lines: brightness from behind the region of the layer ($B'_{\mathrm{sky}/F}$); full lines: total brightness of the sky (B'/F) in direction of the layer; dashed lines: horizontal brightness in pure air.

Horizontal divergence or convergence at the level of a layer may produce such changes, or, hypothetically, the stratification and mixing of two similar layers whose tops were at altitude H and $H-D$. These relations are partly applicable for the conditions of layers in the atmosphere (i.e. including sky background and attenuation) if "brightness" is replaced by "brightness contrast" (see sect. 3.4).

It may be interesting to note that in observing directions, for which the curvature of the layer is not important (e.g. toward zenith), the brightness is independent of layer thickness resp. proportional to the thickness, for the two mentioned cases of $\sigma(D) \sim 1/D$ resp. $\sigma(D) = \mathrm{const.}$

2.5. Determination of layer thickness

Another remark may refer to the practical determination of layer thickness from observations. According to Eq. (2a), the thickness of a layer observed from the altitude of their top is defined by the depression angle δ^* of the direction of maximum geometric path length. Apart from the difficulty to measure this angle (see SIEDENTOPF, 1948) and the possibility of an inclination of the layer, the depression of the direction of maximum path-length (δ^*) is not always identical to the depression of direction of maximum brightness: if the particle distribution is not constant over the vertical extent of the layer (see profile III in Fig. 3), or if the horizontal attenuation in the atmosphere or along the layer is large (as in Fig. 7). However, the half width of a layer brightness profile (δ_h) is fairly similar to δ^*, and it can therefore be used to estimate the layer thickness. Ratios of δ_h/δ^* of the presented profiles (including Figs. 5 to 7) range between 0.7 (Fig. 2, $h = 0$) and 1.3 (Fig. 3, distribution III), so layer thickness determined from Eq. 2a using δ_h instead of δ^* differ by about ± 50 %.

3. Brightness of the sky at horizon of a haze layer

In the atmosphere, a dust layer is always embedded in more or less clean air. The brightness from the direction of the layer is not only affected by the change of the conditions of scattering and attenuation within the region

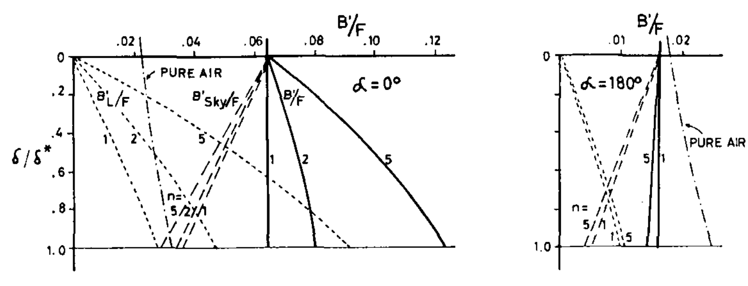

FIG. 6. Same as Fig. 5, but thickness of layer 0.5 km ($\delta^* = 0{,}72°$).

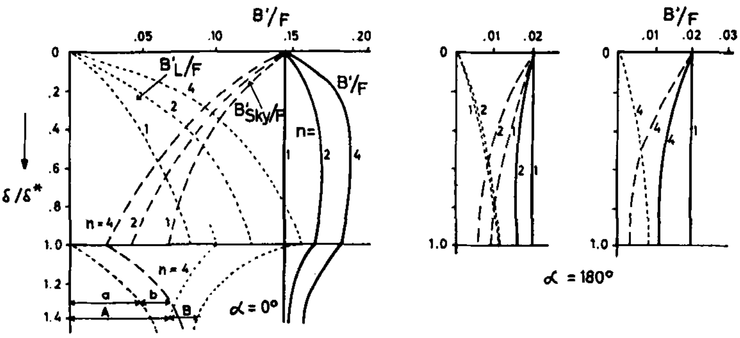

FIG. 7. Same as Fig. 5, but layer at 3 km altitude. At $\alpha = 0$ and for $\delta \geqslant \delta^*$, A (resp. B) shows the brightness contribution of the near (far) branch of the layer $n = 4$, and a (resp. b) shows the contribution of turbid background air ($n = 1$) between (behind) the branches of the layer.

of the layer, but also by the attenuation of the light scattered behind the layer. We will compare the resulting brightness with the brightness of the undisturbed sky at horizon.

3.1. Brightness of the sky at horizon

Neglecting multiple scattering, the sky radiance in a horizontal plane, for depression $\delta = 0$, is generally given by

$$B_{\text{sky}} = \int_a^\infty F(x)\,[\sigma_R(\theta, x) + \sigma_D(\theta, x)]\,T(x)\,dx \qquad (5)$$

with the transmission factor

$$T(x) = \exp - \int_0^x [\underset{R}{\Sigma}(x) + \Sigma_D(x)]\,dx, \qquad (5')$$

where $F(x)$ = intensity (flux) of solar radiation at horizontal distance x from the observer; $\sigma_R(\theta, x)$; $\sigma_D(\theta, x)$ = scattering coefficients of air and dust for scattering angle θ, at x; $\Sigma_R(x)$; $\Sigma_D(x)$ = attenuation coefficients at x.

A solution of (5) for the Rayleigh atmosphere, i.e. generally for an atmosphere with constant scale height γ above the altitude H of the observer, has been derived by SIEDENTOPF (1948):

$$B_{\text{sky}} = F_H \sigma_H(\theta) \sum_{-1}^{H} (1 - e^{-f})$$

with $f = 0.5\ \Sigma_H (2\pi\gamma E)^{\frac{1}{2}}$, i.e. $f = 283\ \Sigma_H$ for $\gamma = 8$ km. σ_H and Σ_H are scattering and attenuation coefficients at H. The saturation brightness

$F_H \sigma_H / \Sigma_H$ is reached for Σ_H larger than about 0.01 km^{-1}.

In our models, however, a slightly turbid atmosphere has been assumed and computations were based on Eq. (5).

3.2. Variation of brightness of the horizon with elevation angle

For comparison of brightness of the sky at horizon and of a layer, we have also to consider the change of sky brightness for small deviations from the horizontal direction. According to the data of Bemporad, the relative path length (M) in a pure atmosphere ($M = 1$ in zenithal direction) can be approximated by the function

$$d \log M / d\delta \approx 0.20 \text{ deg}^{-1}, \quad \text{for } -2° < \delta < 2°. \qquad (7)$$

The value of M is 39.7 at $\delta = 0$, but it may slightly change with refraction condition and altitude, as the factor in (7).

For heights, elevations, and wavelengths for which the atmosphere is optically thin in direction δ (for $\Sigma_R \cdot M(\delta) <$ ca $2 \cdot 10^{-2}$), the brightness gradient $dlg\ B/d\delta$ is identical to the path-length gradient. This holds also for a turbid atmosphere if—as probably in the mesophere—the scale heights of dust and air are similar. Near the ground, the atmosphere is, in the visible part of the spectrum, always optically thick with respect to horizontal brightness. Then, the brightness gradient is very small in the absence of haze inhomogenities.

3.3. Computation of brightness of an atmospheric haze layer

From the direction of the haze layer light is received from the region of the layer and, if

TABLE 2. *Attenuation coefficients (a) and normalized scattering coefficients per radian (b) for λ 500 nm.*

Height (km)	22	3	Scattering angle	20°	140°
(a)			(b)		
$10^3\ \Sigma_R$ (km^{-1})	1.00	12.7	$10^3\ \sigma_R(\theta)/\Sigma_R$	114	85
$10^3\ \Sigma_D$ (km^{-1})	0.41	18.4	$10^3\ \sigma_D(\theta)/\Sigma_D$	360	8

the layer is transparent, from the sky behind it. We will assume that the size distribution (i.e. the scattering function $\sigma_D(\theta)$ of the haze particles within the layer is the same as outside the layer in the slightly turbid air, but that the particle concentration is larger by a factor n.

With the observer again at the top of a layer of rectangular vertical distribution of particle density, the brightness from the region of the layer (B'_L) is then, for $\delta \leqslant \delta^*$, to compute with Eq. (5) and (5′) replacing σ_D by $n\sigma_D$, and Σ_D by $n\Sigma_D$. The limits of x in the integrals are 0 and $S(\delta)$. The brightness from the sky behind the layer (B'_{sky}) is obtained by integrating (5) and (5′) from $S(\delta)$ to ∞ and by multiplying by the transmission $T(\delta)$ of the layer between 0 and $S(\delta)$. The observed brightness is $B' = B' + B'_{\text{sky}}$. Slightly more complicated is the computation of brightness in direction $\delta > \delta^*$ because of the intersection of the layer at $S(\delta)/2$ by clean air. For convenience, the computations by a graphical-numerical method were made with the optical data at depression 0, neglecting the increase of air density (and brightness) with increasing depression as discussed in sect. 3.2.

All models were calculated for solar elevation 20° and for azimuths $\alpha = 0$ and 180°, i.e. scattering angles of $\theta = 20°$ and 140°, and mainly for wavelength 0.5 micron. Attenuation coefficients for 22 and 3 km altitude, and normalized scattering coefficients are given in Tables 2*a* and *b*. The dust attenuation coefficient (Σ_D) is assumed to be constant from 10 to 30 km; its value is consistent with Junge's balloon measurements from about 17 to 23 km. Above 30 km, a constant mixing ratio dust to air was assumed. The turbidity used for 3 km is equivalent to a visibility range of about 130 km. The number of areosol particles per cm^{-3} in the radius range 0.1 to 1 micron is approximately given by $4.3 \cdot 10^3\ \Sigma_D$.

The dust scattering coefficients $\sigma_D(\theta)$ are based on a size distribution $dN/d\lg r \sim r^{-3}$, and a refractive index of $n = 1.5$, but values for other possible size distributions are not much different.

3.4. The brightness profiles of haze layers

Brightness profiles of two layers of altitude 22 km, with thickness $D = 12.5$ m and 0.5 km ($S = 25$ and 160 km), are shown in Figs. 5 and 6, while Fig. 7 is presenting a layer of $D = 12.5$ m at 3 km. Only in Fig. 7 profiles are extending to larger depressions than δ^*. In each example, the ratio of particle density inside and outside of the layer has been varied from 1 (no layer) to values giving medium and high layer brightness. The brightness contribution stemming from the region of the layer (B'_L) is shown by dotted lines, the brightness coming from the sky behind the layer (B'_{sky}) by broken lines, and the resulting brightness (B') by full lines, respectively. The increase of horizontal brightness with increasing depression angle according to Eq. (7) is shown in Figs. 5 and 6 by dashed lines for pure air.

We are now discussing the brightness profiles. At *high altitude*, and for azimuth 0, the brightness of the horizon is 2.8 times larger in the hazy atmosphere than in pure air. At this azimuth, the increase of brightness by the haze of a layer is larger than the reduction of background skylight (B'_{sky}) by the attenuation of the layer. But at $\alpha = 180°$, small haze scattering does not outweigh the increased attenuation so that the resulting brightness, even without a layer, is smaller than in a pure atmosphere.

Comparison of Figs. 5 and 6 shows, that at $\alpha = 0$ and 180°, and for the same particle density ratio (n), the contrast $C(\delta) = B'(\delta)/B(0) - 1$ of the thick layer against the sky is about 5 times larger than for the thin layer. For comparison, the considerations of sect. 2.4 gave $B \sim \sqrt{D}$ for

TABLE 3. *Contrast of layers against the horizon for single scattering (C_s) and with multiple scattering (C_m) for $\eta = 0.2$.*

Layer density (n)	3		11		3	
Layer thickness (D)	500 m		12.5 m		12.5 m	
Altitude (H)	22 km		22 km		3 km	
Scattering angle	20°	140°	20°	140°	20°	140°
C_s	.50	−.02	.41	−.05	.20	−.46
C_m	.48	+.08	.38	+.30	.19	−.35

$\sigma(D) = \text{const}$, so that the brightness ratio of isolated layers would be $\sqrt{500/12.5} = 6.3$. The negative contrasts at $\alpha = 180°$ are only about 1/10 of the contrasts at 0°. With both layers, deformation of the brightness profiles by attenuation is rather small except for the layer of highest value of n ($=100$) in Fig. 5 for which $\Sigma/S^* = 3.2$. The extrapolation of the profiles to $\delta > \delta^*$ is therefore no problem.

The profile of the thin layer has been computed for the additional wavelength 650 nm. Compared to λ 500 nm, the brightness of the horizon is reduced to 40 % in a pure atmosphere and to 70 % for $n = 1$. But contrasts of the layers with $n = 11$ and 100 at depression δ^* are about 30 % higher than at the shorter wavelength. This considerable difference of spectral distribution of radiation gives the layer a white or even brownish color compared to the whitish-blue sky at horizon.

At *3 km altitude*, air and particle density are much higher than at 22 km, but the brightness of the horizon, having now the saturation value $B/F = \sigma/\Sigma$, increases only by a factor 2.1 at $\alpha = 0°$ and by 1.25 at $\alpha = 180°$. The solar illumination F decreased to 59 % of its extraterrestrial value. Due to the strong attenuation in horizontal direction, the sharp brightness maximum at δ^* of the previously discussed layers disappeared and is replaced by a broad maximum at much smaller depression. It is also remarkable that the layer brightness at 180° (compared to the increase at $\alpha = 0$) is much more reduced than at high altitude. The thin layer of 12.5 m thickness gives at altitude 3 and 22 km about the same maximum contrast, if $n = 2$ resp. 11. However, the absolute particle number in the layer is 44 times larger at 3 km than at 22 km.

3.5. MULTIPLE SCATTERING

Up to now, only primary scattering of sunlight has been considered in computing sky and layer brightness. A simple, approximative method to take acount of the additional illumination from the sky and from the direction of the ground (albedo) has been used by SIEDENTOPF (1948). He assumed that the additional illumination, amounting to the fraction η of the direct solar illumination, is independent of direction. The brightness of sky and layer, which in Eq. (5) was proportional to the scattering coefficient $\sigma(\theta)$, would then be proportional to

$$\sigma(\theta) + \eta\bar{\sigma}. \tag{8}$$

$\bar{\sigma} = \Sigma/4\pi$ is the scattering coefficient for anisotropic scattering. With $\eta \approx 0.20$ at 20° solar elevation from measurements by SIEDENTOPF, brightness values of the horizon in the sun's vertical ($\alpha = 0$) increase by 14 % in a pure atmosphere, by 8.3 % in the turbid atmosphere ($n = 1$) at altitude 22 km, and by 6.2 % at 3 km. The relative brightness increase of layers in the sun's azimut is slightly smaller so that at all altitudes contrasts of layers towards the horizon become smaller by about 5 % of the single scattering values (Table 3).

However, at large scattering angles and at high altitude, secondary scattering increases the brightness of a layer much more than that of the sky (40 % at $n = 3$ and 26 % at $n = 1$). Thus, the contrast of a layer with $n = 3$ and 500 m thickness, being -0.02 for single scattering (Fig. 6), becomes $+0.08$. The contrast of a thin layer with high turbidity ($n = 11$, $D = 12.5$ m; Fig. 5) changes from -0.05 to $+0.30$ at azimuth 180° by considering secondary scattering and therefore is nearly constant all along the horizon. This must not mean that conditions for visual observations become independent at azimuth because azimuthal changes of absolute brightness and of color contrast are remaining. SIMONS (1958) observed high altitude layers preferably near the sun's vertical. But in the very turbid lower atmosphere, the effect of multiple scattering is, in agreement with observations, not sufficient to make the layer brighter than the horizon at large scattering angles.

Our assumption of anisotropy of the additional illumination certainly overemphasizes the effect of multiple scattering. Computations by Bullrich, de Bary & Möller (1952, Fig. 11) for ground layer conditions of turbidity show that the backscatter phase function of secondary scattering is only about half of that of forward scattering. Smaller values of the backscattering of the areosol than assumed would also reduce the effect of multiple scattering.

4. Comparison with the zenith brightness method

A relative simple method to determine the vertical distribution of areosol scattering is the measurement of sky brightness from ascending aeroplanes or balloons. The approach of the top of the ground level haze, and the transgression of strong haze layers cause accelerated decrease of zenith brightness (e.g. Tousey & Hulbert, 1941). It is interesting to compare the sensitivity of this method with the effect of a layer on horizontal brightness.

Computations were made on the effect of a layer of 0.5 km thickness at 22 km altitude, with the particle density twice as large as in Table $2a$ (i.e. $n = 2$). For a scattering angle of 20° and at elevation 20°, the sky brightness at the bottom of the layer is 10.5 to 22.5 % larger than without the layer, depending on the turbidity above the layer (constant mixing ratio according to Table $2a$, respective pure air). The zenith brightness ($\theta = 70°$) is decreased by the layer by one per cent only. While the contrast of the same weak layer on the horizon, being 20 % near the sun's vertical at 20° solar elevation, can be easily measured from photographs, zenith brightness measurements require an accuracy of about 1 per mille per km altitude to allow for comparative analysis of details of profile and particle density of the layer. For strong layers, however, showing saturation of horizontal brightness, zenith measurements become more feasible. If the layer thickness decreases, the effect on oblique observation decreases much more than on lateral observation. For $D = 12.5$ m, the ratio of zenithal and horizontal brightness effect would be 1 to $20\sqrt{40} = 1$ to 133, instead of 1 to 20 for $D = 500$ m.

Finally, we may compare the detectability of a stratospheric haze layer by ground-based and airborne searchlight experiments. The scattering angle of ground-based measurements is in the order of 140°, so a brightness increase of 4 per cent is to be expected from the abovementioned layer of 500 m thickness of twice the particle density of the surrounding air, sufficient angular resolution provided. Much better are the prospects to detect a layer of such particle concentration by airborne volume scattering measurements (nephelometer) at a scattering angle of 20°, because scattering would be about twice as large as in surrounding turbid air.

5. Evaluation of a balloon photograph of a stratospheric layer

As already mentioned, Moore (personal communication, 1960) photographed a haze layer at 24 km altitude during a balloon flight on November 28, 1960. He kindly permitted to the author evaluation of the color slide and to publish the results. The 35 mm Kodachrome slide was taken over Wisconsin at noon time (solar elevation about 24°) in the direction of the sun's vertical, with a focal length of 90 mm. It shows a small, white band of haze across the azimuthal field of view (15°). The smallest depression at which some distant clouds can be seen is 3.8° (with respect to the layer); this is corresponding to a cloud ceiling of 10.5 km. Details of the surface of the earth are discernible at depressions larger than 5°, but transmission in the ground layer was too small to show the distant rim of the earth.

A microdensitometer recording taken with a green filter is presented in Fig. 8. The layer is shown clearly with a maximum brightness contrast of about 5 per cent. The half width of the layer is about 0.17°, so the layer thickness was in the order of 30 m (see sect. 2.5) assuming the layer was homogeneous and at the altitude of the observer. If such a layer were at 22 km, the haze attenuation coefficient Σ_D would be about twice as large ($n = 2$) as in normal turbid air ($n = 1$). This can be deduced

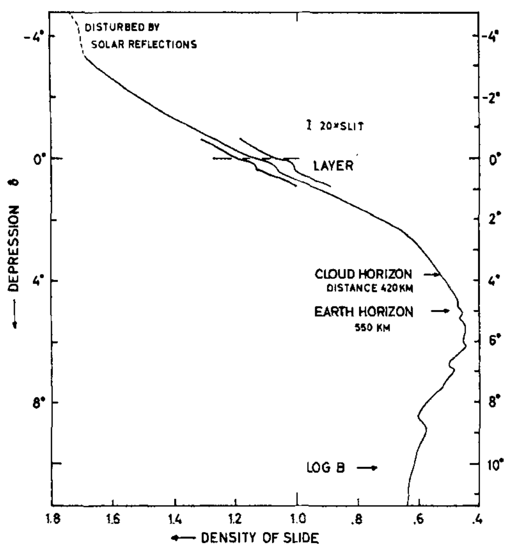

FIG. 8. Haze layer at 24 km. Microdensitometer recording of a color slide taken by Charly Moore on a balloon flight.

from Fig. 5 and Eq. (4) or (4′). Considering smaller background brightness at 24 km due to decrease of air and particle density, the layer may consist of particles in a concentration of the order of 0.5 per cm^3 (see sect. 3.3).

In the neighborhood of the layer, the density gradient of the recording is about -0.23 deg^{-1}, which—under consideration of the unknown gamma value of the uncalibrated film—is in good agreement to the logarithmic path length resp. brightness gradient deduced from the Bemporad function (sect. 3.2).

6. Luminescent layers

The first orbital space flights turned the attention to airglow layers. Circling at a mean altitude of 200 km, GLENN (1962) observed that the night sky was slightly brightened from about 6 to 8° above the earth horizon. Expectations that this glow was caused by the green oxygen line, centered at about 100 km altitude, could be confirmed by CARPENTER (1962) by observing through a λ 5577 narrow band filter. Clearly, the brightness of such luminous layers can be calculated in a similar way as sunlit layers if the vertical distribution of excited atoms is known.

7. Conclusions

An easy and useful method—though neglected and hardly used—to detect and investigate thin and horizontally extended haze layers is by viewing them from airplane or balloon on a horizontal plane. For strong layers ground-base observations of searchlight brightness as well as airborne zenith brightness measurements are more suited. From horizontal observations, the thickness of layers can be obtained directly from their angular width, while estimates on density and vertical profile of particle number become difficult for layers, altitudes and wavelengths, for which horizontal attenuation is large. It would be interesting to extend the present computations to other wavelengths and to compare the color of sky and horizon as function of azimuth and solar elevation. Special attention in observation and model computation should be given to the layer contrast at large distances from the sun with respect to the influence of multiple scattering. In addition, some observers assumed also a considerable influence of light absorption by the aerosol substance.

REFERENCES

BULLRICH, K., DE BARY, E., and MÖLLER, F., 1952, Die Farbe des Himmels. *Geofis. pura appl.*, **23**, pp. 3–44.

CARPENTER, M. S., O'KEEFE, J. A., and DUNKELMAN, L., 1962, Visual observations of nightglow from manned spacecraft. *Science*, **138**, pp. 978–980.

DRIVING, A. YA., and SMIRNOVA, A. I., 1958, Clouds in the stratosphere. *Akad. Nauk SSSR, Ser. Geofiz.*, pp. 337–346.

GLENN, J. H., 1962, The Mercury-Atlas-6 Space Flight. *Science*, **136**, p. 1093.

JACOBS, L., 1954, Dust clouds in the stratosphere. *Met. Mag.*, **83**, pp. 115–119.

JUNGE, C. E., CHAGNON, C. W., and MANSON, J. E., 1961, Stratospheric aerosols. *Journ. Met.*, **18**, pp. 81–108.

LINK, F., 1956, *Die Mondfinsternisse*. Leipzig Akad. Verlag, 127 pp.

LÖHLE, F., 1940, Über die prognostische Bedeutung der Schichtung des Dunstes. *Meteor. Zeitschr.*, **57**, pp. 73–77.

LUDLAM, F. H., 1957, Noctilucent clouds. *Tellus*, **9**, pp. 341–364.

MIKIROV, A. E., 1962, Aerosol scattering coefficient measurements at 80–100 km. *Space Res.* **III**, pp. 155–161.

MOROZOV, V. M., 1957, Non molecular light scattering in the high atmospheric layers. *Met. Soc. Roy. Sci. de Liège*, 4th Ser., **18**, p. 70.

ROESSLER, F., 1961, Messungen des diffusen Himmellichts mittels der Veronique-Rakete. *Wetter u. Leben*, Sonderheft IX, pp. 134–139.

SIEDENTOPF, H., 1948, Optische Erscheinungen an Dunstgrenzen. *Meteor. Rundschau*, **1**, pp. 456–459.

SIMONS, M., 1958, Observations made during Manhigh II Flight. *Jet Propulsion*, **28**, p. 521.

TOUSEY, R., and HULBURT, E. O., 1947, Brightness and polarization of the daylight sky at various altitudes above sea level. *Journ. Opt. Soc. Amer.*, **37**, pp. 78–83.

VOLZ, F. E., and GOODY, R. M., 1962, The intensity of the twilight and upper atmospheric dust. *Journ. Atm. Sci.*, **19**, pp. 385–406.

WALDRAM, F. M., 1945, Measurements of the photometric properties of the upper atmosphere. *Quart. J. R. Met. Soc.*, **71**, pp. 319–325.